Methyl- and methoxy-substituted di[1,4]benzodithiio[2,3-*b*:2,3-*e*]-pyridines as new electron donor compounds: synthesis, molecular structure, electrochemical properties, and EPR studies

B. Bueno,[a] B. Esteve,[b] J. Irurre,[b] E. Brillas,[c] X. Torrelles,[d] J. Rius,[d] A. Alvarez-Larena,[e] J. F. Piniella,[e] C. Alemán[f] and L. Juliá *[a]

[a] *Departament de Química Orgànica Biològica, Centre d'Investigació i Desenvolupament (CSIC), Jordi Girona 18–26, 08034 Barcelona, Spain*
[b] *Departament de Química Orgànica, CETS Institut Químic de Sarrià, Universitat Ramon Llull, 08017 Barcelona, Spain*
[c] *Departament de Química Física, Universitat de Barcelona, Diagonal 647, 08028 Barcelona, Spain*
[d] *Institut de Ciència de Materials (CSIC), Campus de la U.A.B., 08193 Bellaterra, Spain*
[e] *Unitat de Cristallografia, Universitat Autònoma de Barcelona, 08193 Bellaterra, Spain*
[f] *Departament d'Enginyeria Química, ETSEIB, Universitat Politècnica de Catalunya (UPC), Diagonal 647, 08028, Spain*

Received (in Cambridge) 5th January 1999, Accepted 19th May 1999

Two new derivatives of di[1,4]benzodithiino[2,3-*b*:2,3-*e*]pyridine (**5**) tetrasubstituted with methyl (**7**) and methoxy (**8**) groups at the 2,3,9 and 10 positions have been prepared from 2,3,5,6-tetrachloropyridine, by cyclization reaction with the bidentate nucleophiles, 4,5-dimethyl- and 4,5-dimethoxy-benzene-1,2-dithiol. Cyclic voltammograms for the oxidation of both polyheterocyclic compounds **7** and **8** in CH_2Cl_2 exhibit two consecutive redox couples. The first pairs are due to the equilibria between the initial compounds and their radical cations, while in the second couples, the electrogenerated radical cations are in equilibrium with the corresponding dications. Radical cations of these molecules have been generated in fluid solution, by oxidation of the parent compounds with thallium(III) trifluoroacetate in trifluoroacetic acid in the case of **7**, and by irradiation of a CH_2Cl_2 solution containing trifluoroacetic acid (10%) in the case of **8**. Both species were analyzed by electron paramagnetic resonance (EPR). X-Ray analysis of the molecular structures of both **7** and **8** shows a stable chair-shaped conformation with interplanar angles between the phenyl rings and the pyridine ring of 139.9 and 141.4° for **7** and 133.7° for **8**.

Introduction

There is currently a great deal of interest in the design and synthesis of novel organic redox substances.[1,2] The incorporation of polarizable heteroatoms, such as sulfur, within the π-conjugation donor framework is regarded as a good strategy, because they usually show lower ionization potentials than the corresponding hydrocarbons, and they enhance intermolecular interaction.[3–5]

Recently, thianthrenes have gained new interest as components of conducting organic materials, *e.g.* charge transfer salts.[6–10] Thus, the electron-rich derivative 2,3,7,8-tetramethoxythianthrene (**2**) forms 1 : 1 charge transfer complexes with different acceptors,[6–8,10] and one-electron oxidation of thianthrene (**1**) under aprotic conditions with $AlCl_3$–CH_2Cl_2 yields a stable violet radical cation salt.[9]

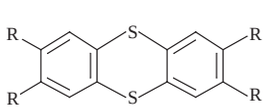

1 R = H
2 R = OCH_3

Planarization of the donor π-system is an important condition for electrical conductivity as it usually facilitates the overlapping of the molecular orbitals. In this context, the molecular structure of thianthrene presents a butterfly shape with a dihedral angle between phenyl groups of 128° in its neutral form, but it is considerably flattened upon removal of one electron to form the stable radical cation.[9] Similarly, while neutral 2,3,7,8-tetramethoxythianthrene is folded along the S · · · S axis, its oxidized radical cation species is planar in the solid salt $[(CH_3O)_2H_2C_6S–SC_6H_2(OCH_3)_2]^{\cdot+}\cdot SbCl_6^-$.[11]

On the other hand, it seems possible to use nonplanar molecules as components of organic conductors if good intermolecular interactions are achieved. Thus 2,3,6,9,10,13-hexamethoxy[1,4]benzodithiino[2,3-*b*]thianthrene (**3**), which

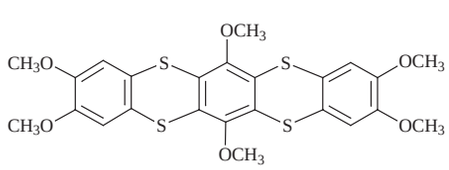

3

can be viewed as two fused thianthrene units and crystallizes in a *trans*-conformation (chain form), acts as a bifunctional donor with 2,3-dichloro-5,6-dicyano-1,4-quinone (DDQ) to form a charge transfer complex with 1 : 2 stoichiometry, each unit being in contact with a DDQ molecule, the donor showing a *cis*-conformation (boat form).[10]

Recently, we have become interested in the synthesis and properties of these tetrathiapolycycles with a pyridine as the central ring, taking advantage in their preparation of the good electrophilic reactivity of 2,3,5,6-tetrachloropyridine (**4**).[12] In this way, we have prepared the novel di[1,4]benzodithiino-[2,3-*b*:2,3-*e*]pyridine (**5**)[12] by reaction of tetrachloropyridine **4** with benzene-1,2-dithiol, and the novel 16-butyldinaphtho-[2′,3′:5,6][1,4]dithiino[2,3-*b*:2,3-*e*]pyridine (**6**)[13] by reaction of 4-butyl-2,3,5,6-tetrachloropyridine with naphthalene-2,3-

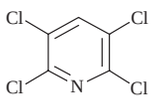

4

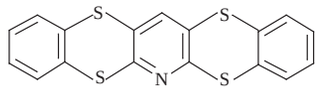

5

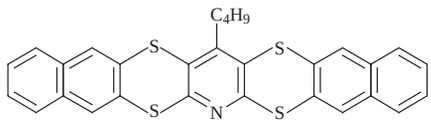

6

dithiol, in dimethylformamide (DMF) and in the presence of an excess of sodium hydrogen carbonate ($NaHCO_3$), with excellent yields. The molecular structures of these neutral pentacyclic molecules show two folds along the S···S lines of the S-containing six-membered rings, with general chair-shaped conformations. The electron paramagnetic resonance spectra of the stable oxidized species, $\mathbf{5}^{\bullet+}$ and $\mathbf{6}^{\bullet+}$, show uniform distributions of the spin-density over the whole molecule, supporting the planarity of the molecules upon one-electron removal.

The poor solubility of **5** in common organic solvents and its moderately high oxidation potential have prompted us to introduce electron donating groups as substituents in the extreme benzo positions. Herein, we report on the synthesis and physical properties of two examples of tetrasubstituted di[1,4]benzodithiino[2,3-*b*:2,3-*e*]pyridines with methyl and methoxy groups in the 2, 3, 9 and 10 positions, as well as preliminary results for their oxidized species as dication salts, and the complexes obtained in fluid solutions with the strong electron acceptor DDQ.

Synthesis

The preparation of the di[1,4]benzodithiino[2,3-*b*:2,3-*e*]pyridines **7** and **8** was performed by reaction of pyridine **4** with 4,5-dimethylbenzene-1,2-dithiol (**9**)[14] and 4,5-dimethoxybenzene-1,2-dithiol (**10**),[15] respectively, using the same method reported for the synthesis of **5**. Thus, pyridine **4** with two equivalents of aromatic dithiol **9** or **10** in DMF and in the presence of an excess of $NaHCO_3$, to generate the sodium salts of the thiols, gave **7** or **8**, respectively, in good yield (Scheme 1).

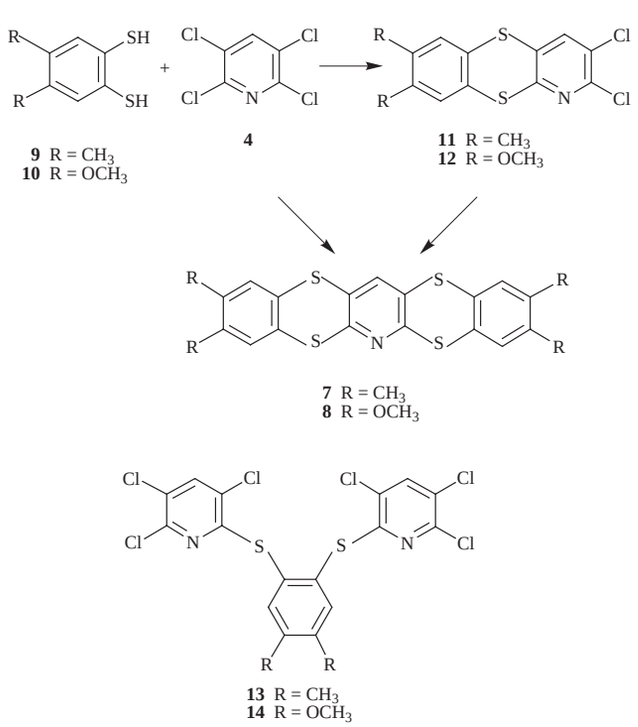

9 R = CH_3
10 R = OCH_3

4

11 R = CH_3
12 R = OCH_3

7 R = CH_3
8 R = OCH_3

13 R = CH_3
14 R = OCH_3

Scheme 1

If equimolecular mixtures of pyridine **4** and dithiol **9** react under similar conditions, 2,3-dichloro-7,8-dimethyl[1,4]benzodithiino[2,3-*b*]pyridine (**11**) is obtained in good yield along with a moderate yield of 2,2′-(4,5-dimethyl-1,2-phenylenedithio)-bis(3,5,6-trichloropyridine) (**13**) as a by-product. Similarly, nucleophilic cyclization of pyridine **4** with dithiol **10** under lower temperature conditions yielded 2,3-dichloro-7,8-dimethoxy[1,4]benzodithiino[2,3-*b*]pyridine (**12**) in good yield, and a small amount of byproduct **14**. Compounds **11** and **12**, as intermediates, react further with more of the sodium salt of thiols **9** and **10** to give **7** and **8**, respectively. Starting from 2,3,5,6-tetrachloropyridine, the isolation of the byproducts **13** and **14** supports the fact that the initial attack on the pyridine **4** takes place at the most reactive 2-position, as was reported for the compound **5**. Dithiols **9** and **10** were prepared according to well-known procedures, starting from *o*-xylene and catechol, respectively, as outlined in Scheme 2.

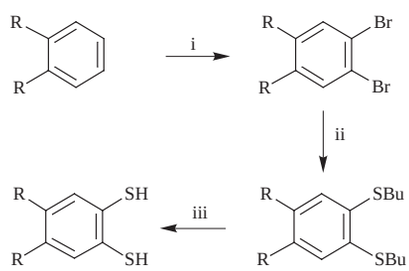

9 R = CH_3
10 R = OCH_3

Scheme 2 *Reagents*: i, Br_2; ii, *n*-BuSCu, quinoline–pyridine; iii, Na, liquid NH_3.

Cyclic voltammetry (CV)

Compound 7. Cyclic voltammograms for the oxidation of compound **7** (0.5×10^{-3} M) in CH_2Cl_2 containing tetra-*n*-butylammonium perchlorate (TBAP) (~ 10^{-1} M) at 25 °C displayed two consecutive redox couples, O_1/R_1 and O_2/R_2, as shown in Fig. 1(b). These two pairs were recorded at scan rates (v) ranging between 20 and 200 mV s^{-1}. The two consecutive oxidation peaks, O_1 and O_2, showed similar heights, indicating that the same number of electrons is involved in both processes. The $|I_p^a|/I_p^c$ ratio for the O_1/R_1 couple (I_p^a = anodic peak current of O_1 peak, I_p^c = cathodic peak current of R_1 peak) was always close to 1. However, the $|I_p^a|/I_p^c$ ratio for the O_2/R_2 couple was only slightly increased from *ca.* 0.4 with increasing v. In addition, the $|I_p^a|/v^{1/2}$ function for both oxidation peaks gradually decreased as v increased. Under these conditions, both couples showed a shift in the anodic peak potential (E_p^a) to more positive values and a shift in the cathodic peak potential (E_p^c) in the cathodic direction. This causes a progressive increase in the difference ($E_p^a - E_p^c$), starting from *ca.* 80 mV at 20 mV s^{-1}. The standard potential $E°$ for each couple was then calculated using $(E_p^a + E_p^c)/2$, remaining largely constant for all v values tested with a precision lower than 10 mV, indicating that the shift in E_p^a and E_p^c with increasing v is mainly due to the quasi-reversibility of the charge transfer processes.

These results agree with the theoretical behaviour expected for quasi-reversible one-electron systems.[16] Thus, **7** undergoes two consecutive charge transfer reactions. The O_1/R_1 couple with standard redox potential $E°_1 = 1.17$ V *vs.* SSCE can be ascribed to the equilibrium reaction between the neutral substrate and its radical cation: $\mathbf{7} \rightleftharpoons \mathbf{7}^{\bullet+} + 1e$. The species $\mathbf{7}^{\bullet+}$ shows great stability in solution, at least during the CV measurements, being the electroactive species of the second oxidation process, where it produces its dication $\mathbf{7}^{2+}$. The O_2/R_2 couple with standard redox potential $E°_2 = 1.37$ V *vs.* SSCE is then due to the equilibrium reaction: $\mathbf{7}^{\bullet+} \rightleftharpoons \mathbf{7}^{2+} + 1e$. The dication $\mathbf{7}^{2+}$ is not as stable as the radical cation $\mathbf{7}^{\bullet+}$ in solution and disappears from the medium, probably *via* hydrolysis with

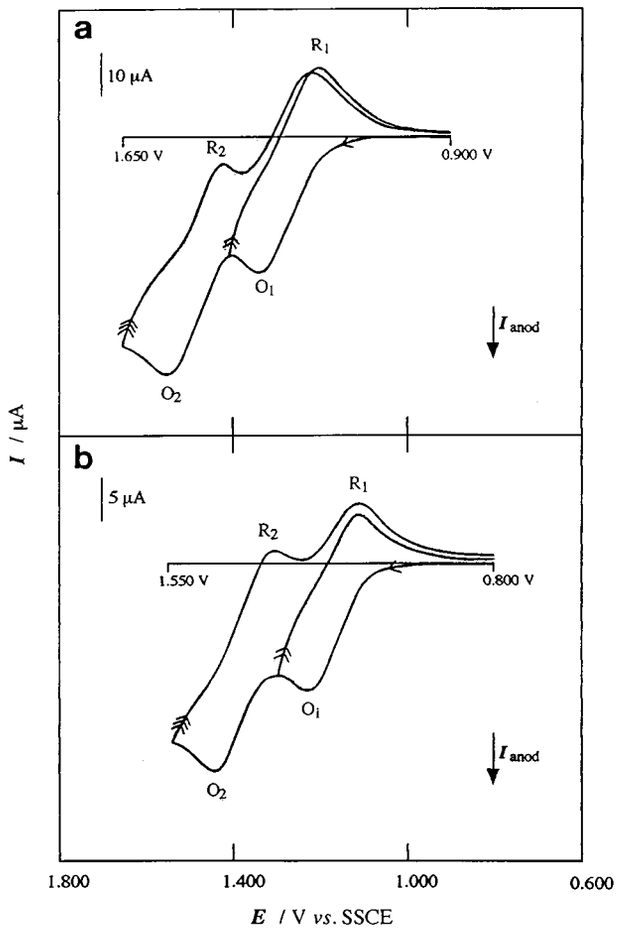

Fig. 1 Cyclic voltammograms for the oxidation of: (a) a 0.5 mM solution of **5** in CH_2Cl_2 with 0.1 M of TBAP on Pt, initial and final potential 0.900 V, reversal potentials (-)) 1.400 V, (-))) 1.650 V; (b) a 0.5 mM solution of **7** in CH_2Cl_2 with 0.1 M of TBAP on Pt, initial and final potential 0.800 V, reversal potential (-)) 1.300 V, (-))) 1.550 V. Scan rate 100 mV s^{-1}. *T* 25 °C.

the trace amounts of water present[17] and/or by precipitation due to its insolubility.

In view of the quasi-reversible behavior observed for the two one-electron redox processes of **7**, Nicholson's theory[18] was applied to calculate the standard rate constants k_s for each couple, according to eqn. (1), where the ψ-parameter for a given

$$k_s = \psi \sqrt{\frac{\pi n F v D}{RT}} \qquad (1)$$

v was taken from the ψ *vs.* $(E_p^a - E_p^c)$ plot calculated by Nicholson for a transfer coefficient $\alpha = 0.5$. The diffusion coefficient D for **7** was assumed to be equal to that of $\mathbf{7}^{\bullet+}$ and $\mathbf{7}^{2+}$. This D value is 2.3×10^{-5} cm^2 s^{-1}, as determined by applying the Randles–Sevcik equation[16] ($|I_p^a| = 2.69 \times 10^5 n^{3/2} A D^{1/2} c v^{1/2}$, where A is the electrode area and $n = 1$) to the O_1 peak at 20 mV s^{-1}, where it shows a better reversibility. From eqn. (1), similar k_s values of $(8.1 \pm 0.3) \times 10^{-3}$ cm^2 s^{-1} and $(6.2 \pm 0.2) \times 10^{-3}$ cm^2 s^{-1} were obtained for the O_1/R_1 and O_2/R_2 couples of **7**.

Compound 8. Cyclic voltammograms for the oxidation of compound **8** (0.5×10^{-3} M) in CH_2Cl_2 containing TBAP ($\sim 10^{-1}$ M) at 25 °C exhibited two consecutive and partially overlapped oxidation peaks, O_1 and O_2, and a small reduction peak R_1, associated with the O_1 peak. In fact, the O_2 and R_1 peaks have similar height and practically disappear at scan rates $v < 50$ mV s^{-1}, increasing in intensities with increasing v. This fact suggests that the electroactive species giving rise to the O_2 and R_1 peaks, which should correspond to the radical cation $\mathbf{8}^{\bullet+}$, is not stable in the medium tested. For this reason, the CV behavior of this compound was investigated in CH_2Cl_2 using *n*-tetrabutylammonium hexafluorophosphate ($TBAPF_6$) (0.1 M) as supporting electrolyte, in the presence of an excess of neutral alumina. This electrolyte was chosen to avoid the possible nucleophilic attack of ClO_4^- anion on $\mathbf{8}^{\bullet+}$, while neutral alumina was added as desiccant.[19] All cyclic voltammograms recorded for a solution of **8** (10^{-3} M) in this medium showed two consecutive O_1/R_1 and O_2/R_2 redox couples, with respective standard potentials $E^\circ_1 = 1.03$ V *vs.* SSCE (similar to 1.05 V found in CH_2Cl_2 with 0.1 M TBAP) and $E^\circ_2 = 1.19$ V *vs.* SSCE. The R_1 and O_2 peaks exhibited similar heights, *ca.* 0.4 times lower than that of the O_1 peak, independent of the scan rate tested. The difference $(E_p^a - E_p^c)$ for both couples was always 80–90 mV. This makes it impossible to determine their corresponding k_s values, since the charge transfers related to the oxidation and reduction peaks of **8** are faster than those of the analogous peaks of **7**. Thus, the O_1/R_1 couple for **8** can be associated with the electrode process: $\mathbf{8} \rightleftharpoons \mathbf{8}^{\bullet+} + 1e$, while its O_2/R_2 pair can be ascribed to the equilibrium reaction: $\mathbf{8}^{\bullet+} \rightleftharpoons \mathbf{8}^{2+} + 1e$. The close proximity between both couples, along with the much lower height of the R_1 and O_2 peaks with respect to that of the O_1 peak, even in the presence of neutral alumina, suggests a real instability of $\mathbf{8}^{\bullet+}$, which could undergo a chemical disproportionation process as follows: $2\ \mathbf{8}^{\bullet+} \rightarrow \mathbf{8} + \mathbf{8}^{2+}$. The dication $\mathbf{8}^{2+}$ is also unstable in the medium: its reduction peak R_2 is only detected in the presence of neutral alumina, indicating its fast hydrolysis with water impurities. In addition, the height of the R_2 peak is not much greater than that of the O_2 peak, suggesting that part of the $\mathbf{8}^{2+}$ formed by oxidation and/or disproportionation of $\mathbf{8}^{\bullet+}$ disappears *via* precipitation due to its low solubility.

Compounds 2 and 5. CV results for the oxidation of compounds **2** and **5** in CH_2Cl_2 with TBAP (0.1 M), under the same conditions as for **7** and **8**, are also reported for the sake of comparison. Compound **2** exhibited two consecutive redox couples. Its first pair, O_1/R_1, was observed at all scan rates, with a standard potential $E^\circ_1 = 0.87$ V *vs.* SSCE (lit.,[7] 0.88 V), and corresponds to the equilibrium reaction: $\mathbf{2} \rightleftharpoons \mathbf{2}^{\bullet+} + 1e$. Although the second oxidation peak O_2 had a similar height to that of the O_1 peak, its concomitant reduction peak R_2 was only detected at a scan rate of 200 mV s^{-1}. This O_2/R_2 couple with $E^\circ_2 = 1.22$ V *vs.* SSCE (lit.,[7] 1.27 V) is related to the electrode process: $\mathbf{2}^{\bullet+} \rightleftharpoons \mathbf{2}^{2+} + 1e$. The disappearance of the R_2 peak at low scan rates is due to the instability of dication $\mathbf{2}^{2+}$, which is probably hydrolysed by water present in the medium.

A typical cyclic voltammogram recorded for **5** is presented in Fig. 1(a). It reveals the presence of two consecutive redox pairs, which behave as quasi-reversible one-electron systems, in a similar way to that described above for the two analogous couples of **7**. While the first couple, O_1/R_1 with $E^\circ_1 = 1.27$ V *vs.* SSCE (lit.,[11] 1.07 V in acetonitrile with $LiClO_4$), related to the process $\mathbf{5} \rightleftharpoons \mathbf{5}^{\bullet+} + 1e$, was recorded for all scan rates tested, the second pair O_2/R_2 with $E^\circ_2 = 1.49$ V *vs.* SSCE, associated with the reaction $\mathbf{5}^{\bullet+} \rightleftharpoons \mathbf{5}^{2+} + 1e$, was only clearly detected above $v = 50$ mV s^{-1}, because the R_2 peak was not observed at lower v values. Note that the O_2 peak for **5** is totally irreversible below 200 mV s^{-1} when recorded in acetonitrile.[12] These results in CH_2Cl_2 and acetronitrile indicate the instability of dication $\mathbf{5}^{2+}$ to reaction with water impurities in the medium. The standard rate constants k_s for the two couples of **5** were also calculated using Nicholson's theory.[17] A D value of 9.4×10^{-5} cm^2 s^{-1} was determined for this compound by applying the Ranles–Sevcik equation[16] to the O_1 peak at 20 mV s^{-1}. Then, from eqn. (1), k_s values of $(8.4 \pm 0.2) \times 10^{-3}$ cm^2 s^{-1} and $(1.11 \pm 0.02) \times 10^{-2}$ cm^2 s^{-1} were calculated for the O_1/R_1 and O_2/R_2 couples of **5**. These k_s values are of the same order of magnitude as those obtained for the analogous couples of **7**, although the diffusion coefficient for **5** is about four times higher than that of **7**, as can be deduced from Fig. 1, because of its smaller size.

Table 1 Standard potentials for the two consecutive couples determined by CV for the oxidation of **5**, **7** and **8**, and tetramethoxythianthrene **2** in CH_2Cl_2 with 0.1 M TBAP at 25 °C

Compound	$E°$/V *vs.* SSCE		
	O_1/R_1 couple	O_2/R_2 couple	$\Delta E°$/V
5	1.27	1.49	0.22
7	1.17	1.37	0.20
8	1.05	—[a]	—
	1.03[b]	1.19[b]	0.16[b]
2	0.87	1.22	0.35

[a] No R_2 peak was observed; [b] Determined in 0.1 M $TBAPF_6$ in presence of neutral alumina.

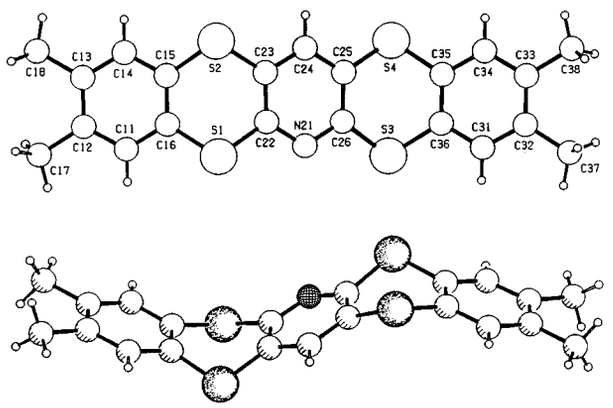

Fig. 2 Molecular structure of **7**.

Table 1 summarizes the standard potentials for the two consecutive redox couples of compounds **5**, **7** and **8**, and of the tetramethoxythianthrene **2**. An analysis of these results for **5**, **7** and **8** suggests that the presence of methyl and methoxy substituents, as electron donors, increases the oxidative ability of both the neutral compounds and their radical cations. This effect is more pronounced in the case of the methoxy substituent than in that of the methyl substituent. The last column of Table 1 shows the difference $\Delta E°$ ($= E_2° - E_1°$) between the standard potentials of both couples. While $\Delta E°$ remains practically constant, close to 0.20 V, on going from **5** to **7**, it decreases significantly in the tetramethoxy derivative **8** as a consequence of the lower intramolecular repulsion (Coulomb energy) between the positive charges in the dication $\mathbf{8}^{2+}$. In addition, this difference for **8** ($\Delta E° = 0.16$ V) is much lower than for 2,3,7,8-tetramethoxythianthrene **2** ($\Delta E° = 0.35$ V), due to the much shorter distance between the positive charges in dication $\mathbf{2}^{2+}$.

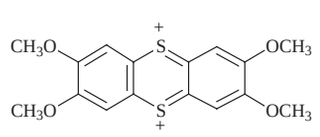

$\mathbf{2}^{2+}$

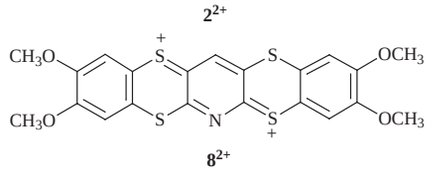

$\mathbf{8}^{2+}$

Molecular structures

Compound 7. The molecular structure of compound **7** is shown in Fig. 2 with the atom numbering scheme. The molecule crystallizes in the monoclinic system, space group $P2_1/n$, with four molecules in the elemental cell. All bond lengths and angles are shown in Tables 2 and 3, respectively. The asymmetric unit is the whole molecule without any crystallographic inversion center. The pyridine and the two benzo rings are planar with rms deviations of 0.009, 0.011 and 0.007 Å, respectively. The two six-membered rings containing the sulfur atoms posses a boat conformation, and the S1, S2, S3 and S4 atoms deviate by 0.017, 0.062, −0.132 and −0.172 Å from the pyridine mean plane, respectively. The folding of the dithiine rings along the S···S axes (dihedral angle between S1–C16–C15–S2 and S1–C22–C23–S2 mean planes) is 133.7(1)°. The pentacyclic molecule has a general chair-shaped conformation with interplanar angles between benzo rings and pyridine of 139.9(1)° and 141.4(1)°.

Table 2 Selected bond lengths for **7**

Atom 1	Atom 2	Bond length/Å
C11	H11	0.930(4)
C11	C12	1.389(4)
C11	C16	1.389(4)
C12	C13	1.404(4)
C12	C17	1.509(4)
C13	C14	1.382(4)
C13	C18	1.512(4)
C14	H14	0.930(4)
C14	C15	1.393(3)
C15	C16	1.388(3)
C15	S2	1.766(3)
C16	S1	1.769(2)
C17	H17A	0.960(6)
C17	H17B	0.960(6)
C17	H17C	0.960(11)
C18	H18A	0.960(8)
C18	H18B	0.960(11)
C18	H18C	0.960(11)
S1	C22	1.761(3)
S2	C23	1.759(2)
N21	C22	1.337(3)
N21	C26	1.335(3)
C22	C23	1.404(3)
C23	C24	1.377(3)
C24	H24	0.930(3)
C24	C25	1.377(3)
C25	C26	1.398(3)
C25	S4	1.762(3)
C26	S3	1.763(2)
S3	C36	1.765(3)
S4	C35	1.768(2)
C31	H31	0.930(4)
C31	C32	1.381(4)
C31	C36	1.387(3)
C32	C33	1.394(4)
C32	C37	1.509(4)
C33	C34	1.394(4)
C33	C38	1.506(4)
C34	H34	0.930(4)
C34	C35	1.382(4)
C35	C36	1.393(3)
C37	H37A	0.960(11)
C37	H37B	0.960(8)
C37	H37C	0.960(10)

Compound 8. The molecular structure of compound **8** is displayed in Fig. 3 with the atom numbering scheme. The molecule crystallizes in the triclinic system, space group $P\bar{1}$ (no. 1), with one molecule in the elemental cell. All bond lengths and angles are shown in Tables 4 and 5, respectively. In this case, the asymmetric unit is half a molecule, and the molecule without a centrosymmetric center possesses a crystallographic inversion center in the middle of the pyridine ring. Positional disorder is present in the molecule, placing the nitrogen in either of the two possible positions with the same probability. The pyridine and the two benzo rings are planar with rms deviations of 0.010 Å

Table 3 Selected bond angles for **7**

Atom 1	Atom 2	Atom 3	Bond angle (°)
C12	C11	C16	121.7(3)
C11	C12	C17	119.9(2)
C11	C12	C13	118.7(2)
C13	C12	C17	121.3(2)
C12	C13	C18	120.6(2)
C12	C13	C14	119.2(2)
C14	C13	C18	120.2(2)
C13	C14	C15	121.8(2)
C14	C15	S2	118.7(2)
C14	C15	C16	118.9(2)
C16	C15	S2	122.3(2)
C11	C16	C15	119.6(2)
C15	C16	S1	122.4(2)
C11	C16	S1	117.9(2)
C16	S1	C22	102.2(1)
C15	S2	C23	101.9(1)
S1	C22	N21	115.3(2)
N21	C22	C23	122.5(2)
S1	C22	C23	122.2(2)
S2	C23	C22	122.2(2)
C22	C23	C24	118.2(2)
S2	C23	C24	119.5(2)
C23	C24	C25	119.8(2)
C24	C25	S4	119.3(2)
C24	C25	C26	118.4(2)
C26	C25	S4	122.1(2)
N21	C26	C25	122.6(2)
C25	C26	S3	122.2(2)
N21	C26	S3	115.1(2)
C26	S3	C36	102.4(1)
C25	S4	C35	102.0(1)
C32	C31	C36	121.7(2)
C31	C32	C37	119.85(2)
C31	C32	C33	119.3(2)
C33	C32	C37	120.9(2)
C32	C33	C38	121.6(2)
C32	C33	C34	119.0(2)
C34	C33	C38	119.4(2)
C33	C34	C35	121.4(2)
S4	C35	C34	118.5(2)
C34	C35	C36	119.5(2)
S4	C35	C36	122.0(2)
C31	C36	C35	119.0(2)
S3	C36	C35	122.3(2)
S3	C36	C31	118.6(2)

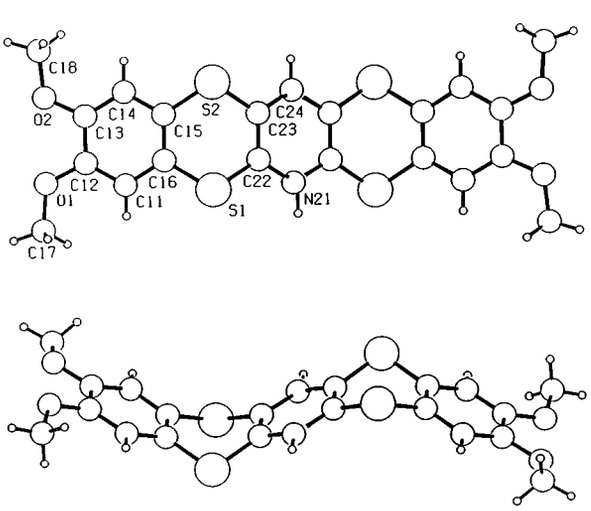

Fig. 3 Molecular structure of **8**.

for the two benzo rings and 0.004 Å for the pyridine. The folding of the dithiine rings along the S · · · S axes, as defined above, is 129.1(1)°. As in the case of **7**, the two six-membered rings containing the sulfur atoms posses a boat conformation, and the S1 and S2 atoms deviate 0.068 and 0.083 Å from the pyridine mean plane, respectively. The pentacyclic molecule has a general chair-shaped conformation with the same value of 133.7° for the interplanar angles between the benzo rings and pyridine.

Table 4 Selected bond lengths for **8**

Atom 1	Atom 2	Bond length/Å
C11	H11	0.970(2)
C11	C12	1.385(3)
C11	C16	1.395(3)
C12	C13	1.411(3)
C12	O1	1.356(3)
C13	C14	1.377(3)
C13	O2	1.362(2)
C14	H14	1.010(3)
C14	C15	1.400(3)
C15	C16	1.382(3)
C15	S2	1.765(2)
C16	S1	1.768(2)
C17	O1	1.423(3)
C17	H17A	0.960
C17	H17B	0.960
C17	H17C	0.960
C18	O2	1.422(3)
C18	H18A	0.960
C18	H18B	0.960
C18	H18C	0.960
S1	C22	1.761(2)
S2	C23	1.763(2)
N21	C22	1.310(3)
N21	C26	1.420(2)
C22	C23	1.394(3)
C23	C24	1.260(3)
C24	H24	0.890(6)
C24	C25	1.440(4)

Table 5 Selected bond angles for **8**

Atom 1	Atom 2	Atom 3	Bond angle (°)
C23	S2	C15	100.93(10)
C22	S1	C16	100.63(9)
C12	O1	C17	117.5(29)
C13	O2	C18	117.7(2)
C22	N21	C23	118.2(18)
C23	C24	C22	120.6(28)
C12	C11	C16	120.1(2)
C13	C14	C15	120.3(29)
O2	C13	C14	125.0(2)
O2	C13	C12	115.1(2)
C14	C13	C12	120.0(2)
C16	C15	C14	119.8(2)
C16	C15	S2	121.7(2)
C14	C15	S2	118.5(2)
C15	C16	C11	120.3(2)
C15	C16	S1	121.3(2)
C11	C16	S1	118.3(2)
O1	C12	C11	125.2(2)
O1	C12	C13	115.3(2)
C11	C12	C13	119.5(2)
C24	C23	C22	122.2(19)
C23	C22	N21	119.8(12)
C24	C23	S2	116.7(19)
C22	C23	S2	121.0(2)
N21	C22	S1	116.2(10)
C23	C22	S1	121.7(2)

Hexachloroantimonate salts of 7^{2+} and 8^{2+}

Compounds **7** and **8** yielded stable dication salts upon oxidation with antimony pentachloride ($SbCl_5$). $SbCl_5$ was added slowly to slightly yellow solutions of substrates in freshly distilled CH_2Cl_2, which were deoxygenated by bubbling argon through them for 5 min. The solutions instantaneously darkened and solids precipitated in excellent yield. From **7**, a green

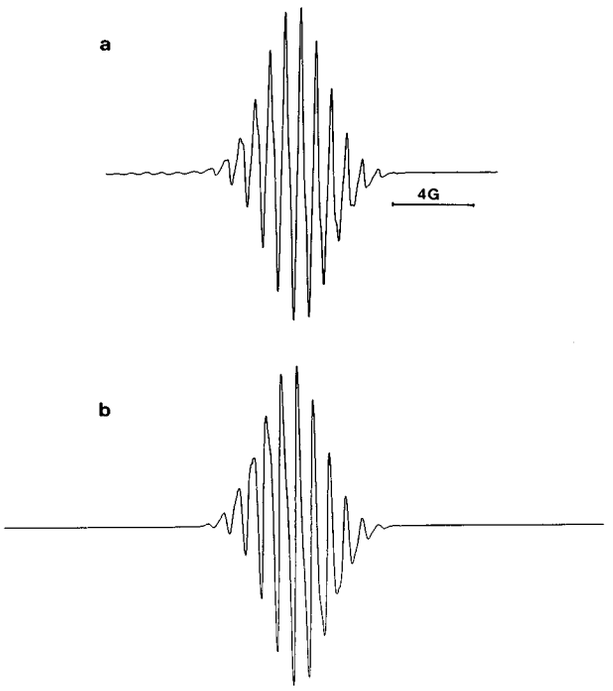

Fig. 4 (a) EPR spectrum of radical cation $\mathbf{7}^{\bullet+}$ generated from a solution of **7** in trifluoroacetic acid containing thallium(III) trifluoroacetate at rt. (b) Computer simulation using the data given in the text.

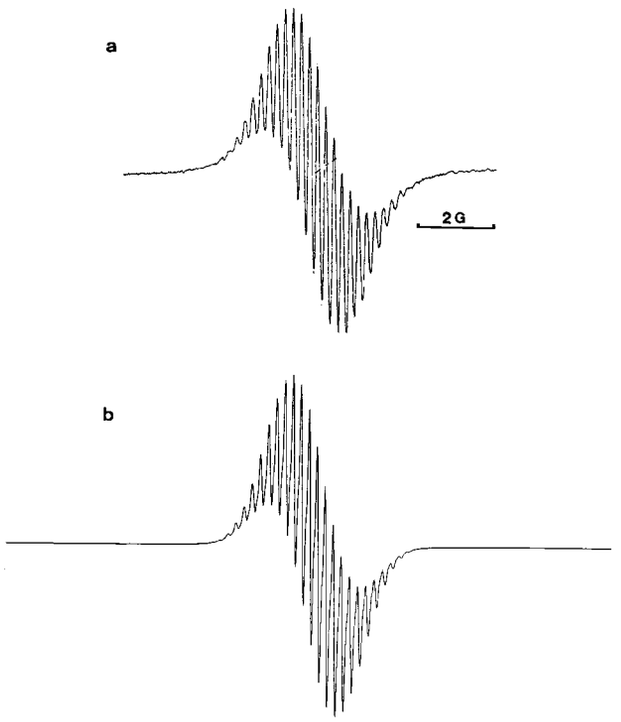

Fig. 5 (a) EPR spectrum of radical cation $\mathbf{8}^{\bullet+}$ generated from an irradiated solution of **8** in CH_2Cl_2 containing trifluoroacetic acid (10%) at rt. (b) Computer simulation using the data given in the text.

solid was separated and characterized as the dication salt $\mathbf{7}^{2+}\cdot 2SbCl_6^-$, and from **8**, a dark brown solid was separated and characterized as the dication salt $\mathbf{8}^{2+}\cdot 2SbCl_6^-$. Both salts are active under EPR analysis displaying under conditions of high amplification single, broad peaks ($\Delta H_{pp} \sim 16.5$ G for $\mathbf{7}^{2+}\cdot 2SbCl_6^-$ and $\Delta H_{pp} \sim 16.2$ G for $\mathbf{8}^{2+}\cdot 2SbCl_6^-$) without any structure, which should correspond to the residual radical cations present at the samples.

Spectral properties of mixtures of 7 and 8 with 2,3-dichloro-5,6-dicyano-1,4-quinone (DDQ)

Preliminary results obtained when the strong electron acceptor 2,3-dichloro-5,6-dicyano-1,4-quinone (DDQ) was added into diluted solutions ($\sim 10^{-2}$ M) of **7** and **8** in $CHCl_3$ indicated the existence of charge transfer complexes. Thus, both substrates in the presence of DDQ developed in their electronic spectra a weak and very broad band with maxima at $\lambda = 749$ nm and $\lambda = 807$ nm for **7** and **8**, respectively. The DDQ charge transfer complex with the unsubstituted species **5** also gave rise to a broad and less intense absorption band, hypsochromically shifted at $\lambda = 705$ nm. Only in the case of **8**, when solutions in CH_2Cl_2 were examined by EPR spectroscopy, a weak signal (g = 2.0072) due to the radical cation $\mathbf{8}^{\bullet+}$ appeared together with the stronger signal ($g = 2.0050$) of the DDQ radical anion. However, all attempts to isolate solid complexes have been unsuccessful so far, only crystalline **8** being separated from those solutions.

Electron paramagnetic resonance (EPR) spectroscopy

A single, broad line ($g = 2.0075$; peak to peak linewidth, $\Delta H_{pp} = 5.75$ G) of a stable radical cation was detected by EPR from a dilute sulfuric acid solution of **7**. A highly resolved EPR spectrum ($g = 2.0077$; $\Delta H_{pp} = 0.08$ G) at room temperature was obtained when degassed solutions of **7** in trifluoroacetic acid were treated with thallium(III) trifluoroacetate. This spectrum was undoubtedly due to $\mathbf{7}^{\bullet+}$ [Fig. 4(a)] and was simulated [Fig. 4(b)] using the following hyperfine splitting (hfs) constant values: $a(1H) = 0.50$ G; $a(1N) = 0.09$ G; $a(12H) = 0.80$ G; $a(4H) = 0.11$ G. The one proton coupling constant value should be assigned to the hydrogen in position 13 in the pyridine ring, and the last value to the four hydrogens in positions 1, 4, 8 and 11. Under conditions of high amplification, the hfs values due to the coupling of the electron with naturally abundant ^{33}S (0.76%) were observed as two multiplet satellite lines [$a(^{33}S) \sim 4.7$ G] which should correspond to the $M_S = \pm 3/2$ groups of the quartet [$I(^{33}S) = 3/2$)], the two $M_S = \pm 1/2$ groups being lost in the envelope of the very intense central multiplet.

Similarly, a single, broad line ($g = 2.0066$; $\Delta H_{pp} = 3.4$ G) of a persistent radical cation was detected from dilute sulfuric acid solutions of **8**. A highly resolved spectrum ($g = 2.0072$; $\Delta H_{pp} = 0.08$ G) was achieved at room temperature after prolonged UV irradiation of degassed solutions of **8** in distilled CH_2Cl_2 containing trifluoroacetic acid (10%) [Fig. 5(a)]. The resolution of the spectrum was not sensitive to lowering of the temperature, and it was analyzed *via* a computer simulation [Fig. 5(b)] using the following hyperfine data: $a(1H) = 0.42$ G; $a(1N) = 0.08$ G; $a(12H) = 0.21$ G; $a(4H) = 0.63$G. This spectrum was attributed to the radical cation $\mathbf{8}^{\bullet+}$ and the assignment of the hfs constants to sets of equivalent nuclei is straightforward: the one proton coupling constant value corresponds to the hydrogen in position 13 and the values for four hydrogens to those in positions 1, 4, 8 and 11. Under conditions of over-modulation and high amplification, the hfs due to coupling with ^{33}S nuclei appeared as two broad satellite lines [$a(^{33}S) \sim 4.2$ G], corresponding to the two $M_S = \pm 3/2$ groups of the quartet, as in $\mathbf{7}^{\bullet+}$. In both radical cations $\mathbf{7}^{\bullet+}$ and $\mathbf{8}^{\bullet+}$, the magnitude of the splitting constant $a(^{33}S)$ is consistent with the value observed for the unsubstituted radical cation $\mathbf{5}^{\bullet+}$, $a(^{33}S) = 4.7$ G.[12]

When the radical cation of the parent compound **5** was obtained and characterized by EPR for the first time, there was an inconsistency in the simulated spectrum, as was pointed out.[12] A thorough and more accurate analysis has prompted us to review and improve its spectral parameters. In Fig. 6, the observed and simulated spectra of $\mathbf{5}^{\bullet+}$ are displayed. The following values have been used in the simulation: $\Delta H_{pp} = 0.18$ G; $a(1H) = 1.0$ G (hydrogen in position 13); $a(1N) = 0.67$ G; $a(4H) = 0.58$ G (hydrogens in positions 2, 3, 9, 10); $a(4H) = 0.13$ G (hydrogens in positions 1, 4, 8, 11).

Table 6 MNDO optimized interplanar angles between benzo rings and pyridine in the neutral **7** and oxidized $\mathbf{7}^{\bullet+}$ and $\mathbf{7}^{2+}$. Experimental X-ray data for the neutral molecule are in parentheses

	Angle (°)		
Ring	**7**	$\mathbf{7}^{\bullet+}$	$\mathbf{7}^{2+}$
Benz 1-Py	160.1 (141.4)	176.8	176.8
Benz 2-Py	159.8 (139.9)	178.3	178.4

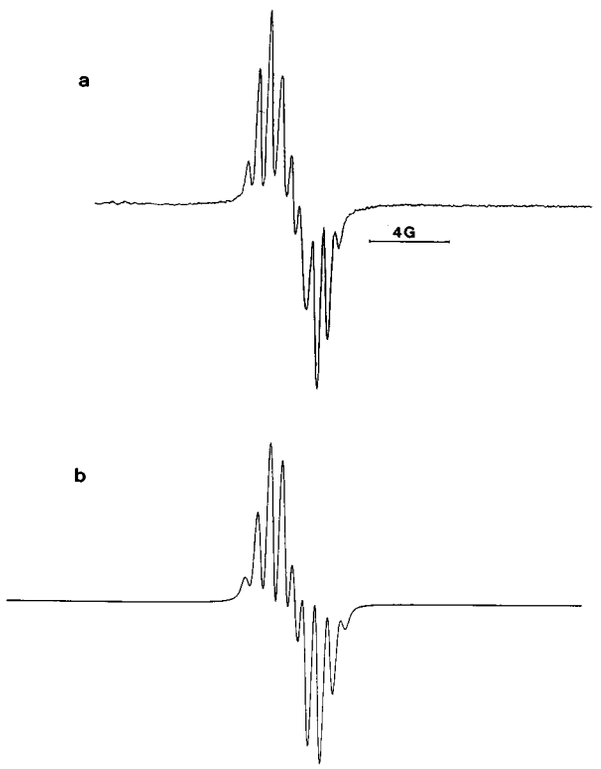

Fig. 6 (a) EPR spectrum of radical cation $\mathbf{5}^{\bullet+}$. (b) Computer simulation using the data given in the text.

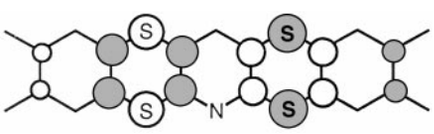

Fig. 7 Electronic structure of the HOMO of **7**.

Theoretical calculations

In order to rationalize the experimental results, the geometrical and electronic structures of **7** were investigated by performing molecular orbital calculations, using the semiempirical MNDO method.[20] In the same way, geometries of the radical cation $\mathbf{7}^{\bullet+}$ and the dication $\mathbf{7}^{2+}$ were also fully optimized by the MNDO method to observe the effects of the oxidation. Fig. 7 shows the atomic coefficients of **7** in the HOMO, indicating that this orbital is mainly located on the two S-containing rings.

Theoretical calculations predict that the minimum energy geometries obtained for the neutral molecule correspond to those in which the molecule is folded in the opposite direction [Fig. 8(a)] or in same direction [Fig. 8(b)] along the S···S axes in each dithiine ring, the second conformation being higher in energy (0.4 kcal mol^{-1}) than the first. This result confirms that obtained by X-ray analysis. In Table 6, the theoretical data for the interplanar angles between the benzo rings and pyridine in the neutral molecule and oxidized species are compared with those obtained from the crystalline structure.

The oxidation process in the molecule mainly affects the dithiine rings, which is in accord with the localization of the HOMO. Thus, the most important effect is the planarization of the molecule which tends to stabilize the radical cation $\mathbf{7}^{\bullet+}$ [Fig. 8(c)] and the dication $\mathbf{7}^{2+}$ [Fig. 8(d)] by extending the conjugation along the whole molecule. In Table 6, the displayed values of the interplanar angles in the oxidized species $\mathbf{7}^{\bullet+}$ and $\mathbf{7}^{2+}$ are practically 180°. This planarization process is made possible by the lengthening and shortening of those bonds in the S-containing rings which correspond in the HOMO to bonding and antibonding character, respectively. The variation of these bond lengths is shown in Table 7, where the values for the dithiine rings of the neutral and oxidized species are collected together with those from the solid state analysis of the neutral molecule. Note that the C–C and C–S bond lengths computed at the MNDO level for the neutral compound are slightly over- and under-estimated, respectively, with respect to the experimental values. However, there is a good correlation between predicted and experimental bond lengths.

Table 7 MNDO optimized bond lengths in the neutral **7** and oxidized $\mathbf{7}^{\bullet+}$ and $\mathbf{7}^{2+}$. Experimental X-ray data for the neutral molecule are in parentheses

	Bond length/Å		
Bonds	**7**	$\mathbf{7}^{\bullet+}$	$\mathbf{7}^{2+}$
C15–C16	1.413 (1.388)	1.421	1.426
C15–S2	1.691 (1.766)	1.682	1.677
S2–C23	1.685 (1.759)	1.657	1.645
C22–C23	1.419 (1.404)	1.447	1.462
C22–S1	1.691 (1.761)	1.664	1.651
C25–C26	1.418 (1.398)	1.447	1.463
C25–S4	1.685 (1.762)	1.659	1.646
S4–C35	1.690 (1.768)	1.681	1.674
C35–C36	1.414 (1.393)	1.420	1.428
S3–C36	1.694 (1.765)	1.690	1.679

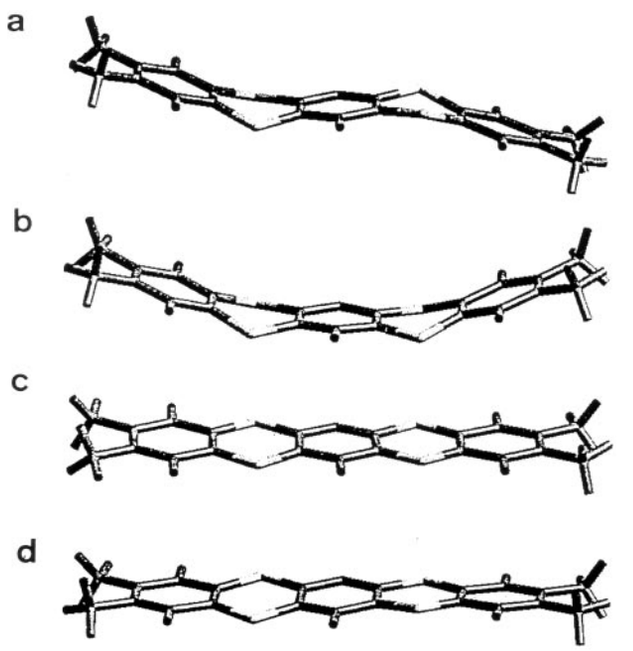

Fig. 8 Minimal energy conformations of the MNDO equilibrium geometries calculated for (a) and (b) **7**, (c) $\mathbf{7}^{\bullet+}$ and (d) $\mathbf{7}^{2+}$.

Summary and conclusions

We have prepared two polyheterocyclic organic compounds **7** and **8** with π-conjugated electronic structures, derived from the novel di[1,4]benzodithiino[2,3-*b*:2,3-*e*]pyridine reported by us recently,[12] as a new class of molecular donors. In both

derivatives **7** and **8**, the solubility in common organic solvents is improved with respect to that of the parent compound. The bidentate nucleophiles benzene-1,2-dithiol **9** and **10** reacted with 2,3,5,6-tetrachloropyridine to give the unsymmetrically substituted species **11** and **12**, respectively, or the symmetrical species **7** and **8**, respectively, depending on the stoichiometries of the substitution reactions.

The X-ray structures of both molecules **7** and **8** show chair-shaped conformations with the two dithiine rings folded in opposite directions along the S···S line. Theoretical calculations performed on **7** predict that the completely planar conformation is about 3.4 kcal mol^{-1} more energetic than the chair-shaped conformation, but when the molecule is oxidized by removal of one or two electrons, the two dithiines are considerably flattened to stabilize the charged species by extending the π-conjugation.

An EPR analysis of the stable radical cations of both molecules, obtained by smooth oxidation in fluid solutions, displays high isotropic *g*-values that indicate a considerable spin–orbit coupling with the sulfur atoms in the molecule. This result is in agreement with the fact that the HOMO is mainly located on the dithiine rings, as is predicted by the semiempirical MNDO method for **7**. The hyperfine structures of the signals in the EPR demonstrate that the singly-occupied molecular orbital (SOMO) in each species is extended over the whole molecule. The values of the free electron coupling with ^{33}S nuclei are approximately half the values observed in the [1,4]benzodithiino[2,3-*b*]pyridine and thianthrene radical cations. This is why **7** and **8** can be properly viewed as two benzodithiinopyridines sharing a common pyridine ring. The four hydrogens in positions 1, 4, 8 and 11 in $\mathbf{8}^{\bullet+}$ are magnetically equivalent in their coupling with the unpaired electron ($a = 0.63$ G), and the twelve hydrogens of the four methyl groups in $\mathbf{7}^{\bullet+}$ also display the same coupling ($a = 0.80$ G). These observations suggest that a pyridine ring instead of a benzo ring does not cause any appreciable asymmetry in the SOMO. A similar observation was made in the thianthrene series when the benzo ring is substituted by a pyridine.[12] In this case, the spectrum of its radical cation consisted of a quartet of lines corresponding to the coupling with the hydrogens in positions 2, 3, 7 and 8. The narrow field range ($\Delta H = 9$ G for $\mathbf{7}^{\bullet+}$ and $\Delta H = 5$ G for $\mathbf{8}^{\bullet+}$) over which the EPR spectra extend is characteristic of these radical cations, and demonstrates once more that the bulk of the spin population resides in the dithiine rings. It is also in accord with the theoretical calculations which locate the HOMO of the neutral molecule mainly in the S-containing rings. If the EPR parameters of $\mathbf{7}^{\bullet+}$ and $\mathbf{8}^{\bullet+}$ are compared with those of the parent radical cation $\mathbf{5}^{\bullet+}$, there is a shifting of the spin density from the pyridine to the external benzo rings, due to the electron donating property of the substituents being greater in $\mathbf{8}^{\bullet+}$ than in $\mathbf{7}^{\bullet+}$.

The values of the standard potentials for the first redox couples in **7** and **8** (Table 1) indicate that these are not particularly strong donors, although the presence of electron-donating substituents decreases their values with respect to the parent compound **5**, particularly when the methoxy group is the substituent. So, a difference of approximately 0.2 V is displayed between the values of the standard potentials of **5** and **8**. Both derivatives **7** and **8** form stable 1:2 ionic salts with $SbCl_6^-$ as the counterion. On the other hand, mixtures of each with DDQ, a strong electron acceptor, in $CHCl_3$ solution show well-defined absorption maxima in the electronic spectra which can be attributed to the presence of charge transfer complexes. EPR spectra of CH_2Cl_2 solutions of **8**, but not of **7**, show a weak signal for the radical cation $\mathbf{8}^{\bullet+}$ together with a stronger one corresponding to the radical anion of DDQ. However, all attempts to isolate a charge transfer complex from **8** and DDQ have failed so far.

Experimental

Melting points were obtained by using a Köfler microscope "Reichert" and are uncorrected. The electronic spectra were recorded with a Perkin-Elmer Lambda Array 3840 spectrometer coupled with a Perkin-Elmer 7300 computer, and the IR spectra with a FT-IR "Bomem-Michalson" model MB-120 spectrophotometer. ^1H NMR spectra were determined at 200 and 300 MHz with Varian Gemini 200HC and 300HC spectrometers, respectively, and ^{13}C NMR spectra at 75 MHz with a Varian Gemini 300HC spectrometer. All the NMR spectra were recorded in $CDCl_3$ with tetramethylsilane as standard. EI mass spectra were obtained on a VG-AutoSpec-Q (Micromass, Manchester) by electron impact at 70 eV; the ion source was set to 200 °C and the current trap was 30 μA.

Dimethylformamide (DMF) was used as received. All the solvents used under anhydrous conditions were dried and distilled before use. $CHCl_3$ and CH_2Cl_2 were dried over calcium chloride, and distilled. Pyridine was dried over potassium hydroxide and distilled, and quinoline was distilled at reduced pressure. Trifluoroacetic acid and sulfur(II) chloride were distilled before use.

4,5-Dimethylbenzene-1,2-dithiol (**9**) was prepared according to the method of Klinsberg:[14] bromination of *o*-xylene gave 4,5-dibromo-*o*-xylene which yielded 1,2-di-*n*-butylthio-4,5-dimethylbenzene by reaction with copper(I) *n*-butanethiolate. Debutylation to the dithiol **9** was accomplished with sodium in liquid ammonia.

4,5-Dimethoxybenzene-1,2-dithiol (**10**) was prepared according to the method of Garner *et al.*:[15] 1,2-dibromo-4,5-dimethoxybenzene was produced by prior dibromination of catechol, followed by methylation of the hydroxy groups with dimethyl sulfate in concentrated aqueous sodium hydroxide. Subsequently, 1,2-dibromo-4,5-dimethoxybenzene was converted into 1,2-di-*n*-butylthio-4,5-dimethoxybenzene by reaction with copper(I) *n*-butanethiolate which yielded dithiol **10** by cleavage of the butyl groups with sodium in liquid ammonia.

Electrochemical measurements

The cyclic voltammetric (CV) experiments were carried out in a three-electrode cell under an argon atmosphere. A Pt disk with an area of 0.093 cm^2 was used as the working electrode and a Pt wire as the counter electrode. The reference electrode was a SSCE (calomel electrode saturated with an aqueous solution of NaCl) connected to the cell through a salt bridge containing a CH_2Cl_2 solution of tetrabutylammonium perchlorate (TBAP) (0.1 M). The temperatures of test solutions and of the SSCE were kept at 25 °C. Solutions of the organic substrates (5×10^{-4} M) in CH_2Cl_2 containing TBAP (0.1 M) as background electrolyte were studied by CV. The volume of all test solutions was 25 mL. CV measurements were performed with standard equipment consisting of a PAR 175 universal programmer, an Amel 551 potentiostat, and a Phillips 8043 X-Y recorder. Cyclic voltammograms of all solutions were recorded at scan rates (v) ranging between 20 and 200 mV s^{-1}.

EPR experiments

EPR spectra were recorded with a Varian E-109 spectrometer working in the X band, using a Varian E-257 temperature controller. Solutions (~ 10^{-3} M) of organic substrates in trifluoroacetic acid (TFA) or mixtures of CH_2Cl_2–TFA, containing thallium(III) trifluoroacetate (TTFA), or in CH_2Cl_2 containing $AlCl_3$ or $SbCl_5$ were placed in quartz EPR tubes, degassed by three freeze-pump-thaw cycles or deoxygenated by bubbling argon through them for 5 min, and then inserted into the EPR cavity. The EPR simulations were carried out with the WinSIM program, received free from The National Institute of Environmental Sciences.

Reaction of 2,3,5,6-tetrachloropyridine (4) and 4,5-dimethylbenzene-1,2-dithiol (1 : 1)

A mixture of 4,5-dimethylbenzene-1,2-dithiol (0.39 g; 2.3 mmol), pyridine **4** (0.5 g; 2.3 mmol), sodium bicarbonate (0.82 g), and DMF (25 mL) was stirred in argon at 100 °C for 2.5 h and then at reflux for 4 h. The mixture was cooled, poured into water, acidified with hydrochloric acid and filtered. The precipitate was chromatographed (silica gel) eluting with CCl_4–$CHCl_3$ (4 : 1) to give: (a) 2,2′-(4,5-Dimethyl-1,2-phenylenedithio)bis-(3,5,6-trichloropyridine) (**13**) (0.01 g, 1.2%); δ_H 7.60 (s, 2H), 7.49 (s, 2H), 2.32 (s, 6 H); δ_C 155.8, 146.2, 139.8, 138.4, 137.8, 131.2, 127.1, 126.1, 19.6 (Found: M 527.8416. $C_{18}H_{10}Cl_6N_2S_2$ requires M^+ 527.8405). (b) 2,3-Dichloro-7,8-dimethyl[1,4]-benzodithiino[2,3-*b*]pyridine (**11**) (0.54 g; 65%), mp 216 °C (from hexane); δ_H 7.72 (s, 1H), 7.22 (s, 1H), 7.21 (s, 1H), 2.23 (s, 6H); δ_C 156.2, 146.6, 137.5, 137.4, 137.0, 131.3, 130.5, 130.0, 129.5, 128.5, 19.2; IR (KBr) ν_{max}/cm^{-1} 2910 (w), 1510 (m), 1470 (m), 1440 (m), 1370 (s), 1350 (s), 880 (m), 870 (m), 670 (w); UV ($CHCl_3$) λ_{max}/nm (ε dm^3 mol^{-1} cm^{-1}) 333.5 (39 000) (Anal. Calc. for $C_{13}H_9Cl_2NS_2$: C, 49.7; H, 2.9; Cl, 22.6; N, 4.4; S, 20.4. Found: C, 49.7; H, 2.9; Cl, 22.6; N, 4.3; S, 20.4%). (c) 2,3,9,10-Tetramethyldi[1,4]benzodithiino[2,3-*b*:2,3-*e*]pyridine (**7**) (0.17 g; 20%), mp 322 °C (from CH_2Cl_2); δ_H 7.62 (s, 1H), 7.22 (s, 2H), 7.19 (s, 2H), 2.21 (s, 12 H); δ_C 156.3, 137.1, 137.0, 134.4, 131.0, 130.0, 129.6, 129.4, 19.3; IR (KBr) ν_{max}/cm^{-1} 2910 (w), 1510 (w), 1470 (m), 1440 (m), 1360 (s), 1350 (s), 890 (m), 870 (m), 860 (m); UV ($CHCl_3$) λ_{max}/nm (ε dm^3 mol^{-1} cm^{-1}) 350 (49 200) (Anal. Calc. for $C_{21}H_{17}NS_4$: C, 61.2; H, 4.1; N, 3.4; S, 31.2. Found: C, 61.2; H, 4.0; N, 3.3; S, 31.2%).

Reaction of 2,3,5,6-tetrachloropyridine (4) and 4,5-dimethylbenzene-1,2-dithiol (1 : 2)

A mixture of 4,5-dimethylbenzene-1,2-dithiol (0.20 g; 1.17 mmol), pyridine **4** (0.13 g; 0.59 mmol), sodium bicarbonate (0.41 g) and DMF (15 mL) was stirred in argon at 100 °C for 1.5 h and then at reflux for 5 h. The mixture was cooled, poured into water, acidified with hydrochloric acid and filtered. The precipitate was chromatographed (silica gel) eluting with $CHCl_3$ to give: (a) 2,3-Dichloro-7,8-dimethyl[1,4]benzodithiino-[2,3-*b*]pyridine (**11**) (0.09 g; 17%). (b) 2,3,9,10-Tetramethyldi-[1,4]benzodithiino[2,3-*b*:2,3-*e*]pyridine (**7**) (0.27 g; 55%).

Reaction of 2,3-dichloro-7,8-dimethyl[1,4]benzodithiino[2,3-*b*]-pyridine (11) and 4,5-dimethylbenzene-1,2-dithiol (1 : 1)

A mixture of 4,5-dimethylbenzene-1,2-dithiol (0.35 g; 2.02 mmol), **11** (0.53 g; 1.70 mmol), sodium bicarbonate (0.73 g) and DMF (25 mL) was stirred under argon at 100 °C for 1.5 h and then at reflux for 5 h. The mixture was cooled, poured into water, acidified with hydrochloric acid and filtered. The precipitate was chromatographed (silica gel) eluting with $CHCl_3$ to give 2,3,9,10-tetramethyldi[1,4]benzodithiino[2,3-*b*:2,3-*e*]pyridine (**7**) (0.41 g; 74%).

Reaction of 2,3,5,6-tetrachloropyridine (4) and 4,5-dimethoxybenzene-1,2-dithiol (1 : 1)

A mixture of 4,5-dimethoxybenzene-1,2-dithiol (0.1 g; 0.50 mmol), pyridine **4** (0.08 g; 0.37 mmol), sodium bicarbonate (0.17 g) and DMF (10 mL) was stirred in argon at room temperature for 5 h. The mixture was cooled, poured into water, acidified with hydrochloric acid and filtered. The precipitate was chromatographed (silica gel) eluting with $CHCl_3$ to give: (a) 2,2′-(4,5-Dimethoxy-1,2-phenylenedithio)bis(3,5,6-trichloro-pyridine) (**14**) (31 mg; 30%), mp 249–252 °C (from benzene); δ_H 7.62 (s, 2H), 7.24 (s, 2H), 3.94 (s, 6H); δ_C 156.6, 150.4, 146.3, 137.9, 127.0, 126.2, 126.1, 119.6, 56.2; IR (KBr) ν_{max}/cm^{-1} 3050 (w), 3005 (w), 2950 (w), 2920 (m), 2840 (w), 1585 (m), 1550 (m), 1500 (s), 1460 (w), 1445 (w), 1430 (m), 1370 (s), 1355 (s), 1325 (m), 1310 (m), 1260 (s), 1225 (m), 1205 (s), 1175 (w), 1145 (s), 1050 (s), 1025 (m), 920 (w), 890 (m), 845 (m), 785 (m), 740 (w), 705 (m), 665 (w), 640 (m), 620 (w). (Anal. Calc. for $C_{18}H_{10}Cl_6N_2O_2S_2$: C, 38.4; H, 1.8; Cl, 37.8; N, 5.0; S, 11.4. Found: C, 38.6; H, 1.8; Cl, 37.7; N, 4.9; S, 11.4%). (b) 2,3-Dichloro-7,8-dimethoxy[1,4]benzodithiino[2,3-*b*]pyridine (**12**) (68 mg; 53%), mp 251–253 °C (from benzene); δ_H 7.76 (s, 1H), 6.97 (s, 1H), 6.95 (s, 1H), 3.88 (s, 6H); δ_C 156.5, 149.6, 149.5, 146.8, 131.6, 128.7, 125.2, 123.1, 112.2, 111.8, 56.3; IR (KBr) ν_{max}/cm^{-1} 3030 (w), 2960 (w), 2930 (w), 2900 (w), 2840 (w), 1580 (s), 1510 (s), 1485 (s), 1455 (s), 1440 (s), 1425 (s), 1380 (m), 1365 (s), 1350 (s), 1335 (s), 1300 (s), 1255 (s), 1205 (s), 1175 (m), 1160 (m), 1070 (m), 1030 (s), 900 (m), 880 (m), 850 (s), 785 (m), 725 (m), 670 (m), 625 (m); UV ($CHCl_3$) λ_{max}/nm (ε, dm^3 mol^{-1} cm^{-1}) 252 (29 200) (Anal. Calc. for $C_{13}H_9Cl_2NO_2S_2$: C, 45.1; H, 2.6; Cl, 20.5; N, 4.0, S, 18.5. Found: C, 45.0; H, 2.5; Cl, 20.6, N, 4.0, S, 18.5%).

Reaction of 2,3,5,6-tetrachloropyridine (4) and 4,5-dimethoxybenzene-1,2-dithiol (2.5 : 1)

A mixture of 4,5-dimethoxybenzene-1,2-dithiol (1.0 g; 5.0 mmol), pyridine **4** (0.43 g; 2.0 mmol), sodium bicarbonate (1.44 g) and DMF (55 mL) was stirred in argon at 100 °C for 1.5 h and then at reflux for 5 h. The mixture was cooled, poured into water, acidified with hydrochloric acid and extracted with $CHCl_3$. The organic solution, washed with an excess of water, dried over Na_2SO_4 and distilled at reduced pressure, yielded a residue which was chromatographed (silica gel) eluting with $CHCl_3$ to give 2,3,9,10-tetramethoxydi[1,4]benzodithiino[2,3-*b*:2,3-*e*]pyridine (**8**) (0.56 g; 60%), mp 305–307 °C (from hexane); δ_H 7.69 (s, 1H), 6.97 (s, 2H), 6.94 (s, 2H), 3.87 (s, 6H), 3.86 (s, 6H); δ_C 156.8, 149.4,149.3, 139.6, 130.0, 125.8, 123.9, 112.2, 111.7, 56.2; IR (KBr) ν_{max}/cm^{-1} 3060 (vw), 3000 (w), 2935 (w), 2900 (w), 2835 (w), 1585 (m), 1490 (s), 1460 (w), 1430 (m), 1355 (s), 1340 (s), 1295 (w), 1260 (s), 1215 (s), 1180 (m), 1150 (w), 1120 (m), 1030 (s), 925 (w), 890 (w), 850 (m), 830 (w), 790 (m), 740 (w), 680 (m); UV ($CHCl_3$) λ_{max}/nm (ε/dm^3 mol^{-1} cm^{-1}) 278 (43 300), 258 (38 700) (Anal. Calc. for $C_{21}H_{17}NO_4S_4$: C, 53.0; H, 3.6; N, 2.9; O, 13.5; S, 26.9. Found: C, 53.3; H, 3.6; N, 2.8; O, 13.5; S, 26.2%).

Reaction of 2,3-dichloro-7,8-dimethoxy[1,4]benzodithiino[2,3-*b*]-pyridine (12) and 4,5-dimethoxybenzene-1,2-dithiol (1 : 1)

A mixture of 4,5-dimethoxybenzene-1,2-dithiol (0.10 g; 0.52 mmol), **12** (0.15 g; 0.43 mmol), sodium bicarbonate (0.25 g) and DMF (15 mL) was stirred under argon at 110 °C for 8 h. The mixture was cooled, poured into water, acidified with hydrochloric acid and filtered. The precipitate was chromatographed (silica gel) eluting with $CHCl_3$ to give 2,3,9,10-tetramethoxydi[1,4]benzodithiino[2,3-*b*:2,3-*e*]pyridine (**8**) (0.06 g; 30%).

X-ray analysis of 2,3,9,10-tetramethyldi[1,4]benzodithiino-[2,3-*b*:2,3-*e*]pyridine (7) and 2,3,9,10-tetramethoxydi[1,4]benzo-dithiino[2,3-*b*:2,3-*e*]pyridine (8)

Suitable crystals of **7** were grown by slow vapor diffusion of *n*-hexane into a CH_2Cl_2 solution of the substrate, and crystals of **8** were obtained by slow crystallization from a benzene solution of the substrate. Crystal, experimental and refinement data for **7** and **8** are presented in Table 8. Crystals were mounted in an Enraf-Nonius CAD4 diffractometer with graphite monochromated Mo-Kα radiation (λ = 0.71069 Å) and the ω-2θ scan method was used. Cell parameters were determined from refinement of 25 centered reflections. Structures were solved by direct methods using SumF-TF[21] for **8** and SHELXS-86[22] for **7**, and refined on F^2 for all reflections using the SHELXL-93 program.[23] Non-hydrogen atoms were refined anisotropically. Hydrogen atoms were placed in calculated positions and their isotropic temperature factors were refined. CCDC 188/168. See

Table 8 Crystal data and structure refinement for **7** and **8**[a]

Empirical formula	$C_{21}H_{17}NS_4$	$C_{21}H_{17}NO_4S_4$
Formula weight	411.60	475.60
T/K	293(2)	293(2)
Crystal system	Monoclinic	Triclinic
Space group	$P2_1/n$	$P\bar{1}$
Unit cell dimensions		
a/Å	8.100(1)	4.881(1)
b/Å	12.520(3)	9.764(1)
c/Å	18.733(3)	11.582(1)
α(°)	90	70.542(8)
β(°)	95.22(1)	88.603(8)
γ(°)	90	85.520(8)
V/Å^3	1891.9(6)	518.86(13)
Z	4	1
μ/mm^{-1}	0.507	0.488
F(000)	856	246
Unique reflections	3325	3121
Final *R* indices		
$R(F)$ [$I > 2\sigma(I)$]	0.0358	0.0443
$R(R)$ (all data)	0.0689	0.0944
$Rw(F^2)$ [$I>2\sigma(I)$]	0.0875	
(all data)	0.0913	0.1148

[a] $w = [\Sigma\sigma^2(F_o^2) + (aP)^2 + bP]^{-1}$; where $P = [\mathrm{Max}(F_o^2,0) + 2F_c^2]/3$.

http://www.rsc.org/suppdata/p2/1999/1503 for crystallographic data in .cif format.

Hexachloroantimonate salts of 7^{2+} and 8^{2+}

From 7. To a stirred solution of **7** (0.10 g; 0.24 mmol) in anhydrous CH_2Cl_2 (20 mL) under an argon atmosphere at room temperature neat $SbCl_5$ (0.15 mL; 0.98 mmol) was slowly added. The solution immediately turned deep green, and a powdered green solid precipitated. The resultant mixture was kept for 2.5 h, and the precipitate was filtered and washed thoroughly with an excess of CH_2Cl_2. The solid was dried to afford a green solid (0.26 g; 98%) (Anal. Calc. for $C_{21}H_{17}NS_4Cl_{12}Sb_2$: C, 23.3; H, 1.6; N, 1.3; S, 11.8; Cl, 39.3. Found: C, 23.2; H, 1.7; N, 1.3; S, 11.6; Cl, 36.9%).

From 8. To a stirred solution of **8** (0.091 g; 0.19 mmol) in anhydrous CH_2Cl_2 (15 mL) under an argon atmosphere at room temperature, neat $SbCl_5$ (0.12 mL; 0.94 mmol) was slowly added. The solution immediately turned deep brown, and a powdered dark solid precipitated. The resultant mixture was kept for 2 h, and the precipitate was filtered and washed thoroughly with an excess of CH_2Cl_2. The solid was dried to afford a dark brown solid (0.215 g; 97%) (Anal. Calc. for $C_{21}H_{17}NO_4S_4Cl_{12}Sb_2$: C, 22.0; H, 1.5; N, 1.2; S, 11.2; Cl, 37.2. Found: C, 20.1; H, 1.5; N, 1.2; S, 9.8; Cl, 37.5%).

Acknowledgements

Support of this research by DGICYT of MEC (Spain) through project PB96–0836, and by the "Generalitat de Catalunya" (Grant: GRQ93–8036) is gratefully acknowledged. J. S. thanks the "Generalitat de Catalunya" for a doctoral scholarship. The authors express their gratitude to the EPR service of Centre d'Investigació i Desenvolupament (CSIC) in Barcelona.

References

1 *Introduction to Molecular Electronics*, ed. M. C. Petty, M. R. Bryce and D. Bloor, Edward Arnold, London, 1995.
2 *Proceedings of the International Conference on Science and Technology of Synthetic Metals* (ICSM'94), Seoul, Korea, 1994, published in *Synth. Met.*, 1995, **69–71.**
3 J. M. Williams, *Acc. Chem. Res.*, 1985, **18**, 261.
4 M. R. Bryce, *Chem. Soc. Rev.*, 1991, **20**, 355.
5 T. Jorgensen, T. K. Hansen and J. Becher, *Chem. Soc. Rev.*, 1994, **23**, 41.
6 W. Hinrichs, P. Berges, G. Klar, E. Sánchez-Martínez and W. Gunsser, *Synth. Met.*, 1987, **20**, 357.
7 H. Bock, A. Rauschenbach, K. Ruppert and Z. Havlas, *Angew. Chem., Int. Ed. Engl.*, 1991, **30,** 714.
8 S. Hünig, K. Sinzger, R. Bau, T. Metzenthin and J. Salbeck, *Chem. Ber.*, 1993, **126**, 465.
9 H. Bock, A. Rauschenbach, Ch. Näther, M. Kleine and Z. Havlas, *Chem. Ber.*, 1994, **127**, 2043.
10 P. Berges, V. Mansel and G. Klar, *Z. Naturforsch.*, *Teil B*, 1992, **47**, 211.
11 G. Klar, W. Hinrichs and P. Berges, *Z. Naturforsch.*, *Teil B*, 1987, **42**, 169.
12 C. Martí, J. Irurre, A. Alvarez-Larena, J. F. Piniella, E. Brillas, Ll. Fajarí, C. Alemán and L. Juliá, *J. Org. Chem.*, 1994, **59**, 6200.
13 C. Troya, A. Vidal, E. Brillas, J. Sañé, J. Rius, J. Irurre and L. Juliá, unpublished results.
14 E. Klinsberg, *Synthesis*, 1972, 29.
15 N. D. Lowe and C. D. Garner, *J. Chem. Soc.*, *Dalton Trans.*, 1993, 2197.
16 *Fundamentals of Electrochemical Analysis*, ed. Z. Galus, Horwood, Chichester, 1976.
17 *Organic Electrochemistry. An Introduction and a Guide*, ed. H. Lund and M. M. Baizer, Marcel Dekker, New York, 1991.
18 R. S. Nicholson, *Anal. Chem.*, 1965, **37**, 1351.
19 O. Hammerich and V. D. Parker, *J. Am. Chem. Soc.*, 1974, **96**, 4289.
20 M. J. S. Dewar and W. Thiel, *J. Am. Chem. Soc.*, 1977, **99**, 4899.
21 J. Rius, *Acta Crystallogr.*, *Sect. A*, 1993, **49**, 406.
22 G. M. Sheldrick, *SHELXS-86*, *Crystallographic Computing 3*, ed. G. M. Sheldrick, C. Krüger and R. Goddard, Oxford University Press, England, 1985, pp. 175–189.
23 *SHELXL-93*, *A program for the refinement of crystal structures*, ed. G. M. Sheldrick, Göttingen University, 1993.

Paper 9/00148D